

INFLUENCE OF NITROGEN PRESSURE ON THE ADHESION AND SCRATCH FAILURE MECHANISMS OF TiMoN/NbN MULTILAYER COATINGS DEPOSITED BY CATHODIC ARC PVD

 O.V. Maksakova^{1*},  V.M. Beresnev¹,  S.V. Lytovchenko¹,  M. Sahul²,  M. Čaplovičova³,
 R.S. Galushkov¹

¹V.N. Karazin Kharkiv National University, 4, Svobody Sq., 61000 Kharkiv, Ukraine

²Institute of Materials Science, Slovak University of Technology in Bratislava, 25, Jána Bottu Str., 917 24 Trnava, Slovakia

³Centre for Nanodiagnostics of Materials, Slovak University of Technology in Bratislava, Vazovova 5, 812 43 Bratislava, Slovakia

*Corresponding Author e-mail: o.maksakova@karazin.ua

Received December 15, 2025; revised January 18, 2026; accepted February 2, 2026

Multilayer nitride coatings are widely used to improve the mechanical performance and durability of engineering components subjected to severe tribological loading. In the present work, the adhesion behaviour and failure mechanisms of nanolayered TiMoN/NbN multilayer coatings deposited by cathodic arc PVD were investigated as a function of nitrogen working pressure. Two coatings were synthesized at nitrogen pressures of 0.52 Pa and 0.13 Pa under otherwise identical deposition conditions. Microscopy analysis revealed that both coatings exhibit a well-defined nanolayered architecture consisting of alternating TiMoN and NbN layers with a modulation period of approximately 85 nm and a total thickness of about 9.5 μm . The decreasing of nitrogen pressure results in a higher density of macroparticles due to the longer mean free path of cathodic arc plasma species. Scratch adhesion tests performed under progressive loading conditions allowed identification of two characteristic failure events corresponding to buckling crack initiation and buckling spallation. The multilayer coating deposited at 0.13 Pa demonstrated slightly improved resistance to crack initiation (5.41 N) compared with the multilayer coating deposited at 0.52 Pa (4.72 N). However, both coatings exhibited similar values of the second critical load (12.4–12.5 N). The multilayer coating deposited at higher nitrogen pressure mainly undergoes adhesive failure with extensive substrate exposure. In contrast, the multilayer coating deposited at lower nitrogen pressure exhibits predominantly cohesive damage within the multilayer structure. The obtained results demonstrate that nitrogen pressure during cathodic arc deposition significantly affects the microstructure evolution and the mechanisms of adhesion failure in TiMoN/NbN multilayer coatings. The study provides insight into the optimization of deposition parameters for improving the mechanical reliability of multilayer nitride coatings.

Keywords: PVD; Nitrides; Multilayer coatings; TiMoN; Microstructure; Composition; Adhesion

PACS: 68.55.Jk, 68.65.Ac

1. INTRODUCTION

The adhesion strength of protective coatings is a crucial parameter that determines their actual performance. It is specifically the coating's ability to maintain a strong bond with the substrate under mechanical, thermal, and chemical stresses that influences the service life of a tool or component. For nitride PVD coatings (such as TiN, NbN, MoN, as well as CrN, ZrN, and others), adhesion is affected not only by the natural chemical affinity between the metal or nitride and the substrate but also by several factors: the energy of ion bombardment on the substrate, the level and type of residual stresses, the presence of transition layers (like Ti, TiN, Nb-enriched interlayers), and the hardness-to-elastic modulus ratio (H/E , H^3/E^2), which impacts resistance to crack initiation and propagation.

For example, for the MoN/TiN system it has been shown that a multilayer architecture with a Ti sublayer and a graded transition TiN layer allows the formation of a dense, fine-grained structure with high H/E and H^3/E^2 ratios, which directly correlates with increased adhesion strength in the Rockwell determine their actual performance: it is precisely the coating's ability test compared with monolayer TiN and MoN coatings [1]. For NbN coatings on austenitic steel AISI 316L it has been shown that reactive magnetron sputtering followed by controlled oxidation forms a multiphase NbN/Nb₂O₅ structure with increased microhardness and corrosion resistance; at the same time, cross-sectional polishing and indentation tests demonstrate preservation of the integrity of the “coating–steel” interface, that is, adhesion remains sufficient even after heat treatment [2]. Similarly, in the NbN/Ti system, it has been found that optimization of the N₂ flow rate during magnetron sputtering allows control of the stoichiometry and texture of NbN, which leads to increased conductivity and corrosion resistance of Ti bipolar plates without degradation of their mechanical integrity, that is, due to the formation of a dense, well-adhered interface [3].

The combination of these results shows that even for simple binary nitrides such as TiN, NbN, and MoN, achieving high adhesion is not a trivial task of interface engineering rather than merely the selection of the correct chemical system.

Against this background, interest is growing in alloyed and ternary nitrides based on Ti, Nb, and Mo, which combine high hardness and thermal stability with improved adaptation to substrate deformation. For TiNbN coatings deposited by cathodic arc evaporation on D2 tool steel, Gonzalez-Carmona et al. showed that varying the substrate temperature during deposition leads to the evolution of the FCC phase structure, changes in the lattice parameter, and changes in crystallite shape, which in turn significantly affect adhesion [4]. According to nanoindentation and scratch test data, the optimal

temperature range ensures not only maximum hardness, but also increased H/E and H^3/E^2 ratios, as well as higher critical failure loads L_c ; at the same time, the damage mode changes from purely adhesive delamination to mixed cohesive–adhesive failure, which indicates strengthening of the interface.

For NbN layers used as adhesion interlayers or components of multilayer structures, it has been shown that their dense, fine-crystalline structure and ability to form oxide barrier phases (Nb_2O_5) additionally stabilize the “coating–metal” contact under corrosion and cyclic loading [2,5]. Another important example is the MoN/TiN multilayer, where the alternating layers based on Mo and Ti allow reduction of stress concentration at the interface, improvement of crack resistance, and provide somewhat higher adhesion compared with monolayer analogues; in this case, the Mo phase additionally contributes to lowering the friction coefficient due to the formation of lubricating MoO_3 oxides [1].

Particular attention in recent years has been devoted to TiMoN coatings, where molybdenum is introduced as an alloying element into the TiN matrix. In the work of Van Meter et al. on TiMoN films deposited by PEALD on different substrates, it was shown that wear resistance and adhesion behavior are closely related to interface engineering: control of the thickness and composition of the oxide layer at the “coating–substrate” interface makes it possible to significantly reduce the wear rate and avoid premature delamination [6]. In combination with the TiNbN results, this indicates that alloying TiN with Nb or Mo atoms and constructing multilayer systems based on Ti–Mo–Nb not only modifies the strengthening mechanism (solid-solution, dislocation, interfacial), but also allows deliberate control of adhesion through optimization of residual stresses, texture, and the gradient of properties from the substrate to the surface. That is why in further work it is logical to focus on Ti–Mo–NbN systems, where each of the elements has already demonstrated the ability to improve adhesion both in binary (TiN, NbN, MoN) and ternary (TiNbN, TiMoN) coatings, and their combination in multilayer architectures provides the potential for further enhancement of adhesion strength without loss of hardness and wear resistance.

Multilayer nitride coatings are considered as the next step compared with simple binary and ternary systems, since the periodic alternation of layers with different mechanical and chemical properties makes it possible to simultaneously increase hardness, crack resistance, and adhesion strength to the substrate due to stress redistribution and blocking of crack propagation at numerous interfaces [7,11]. In particular, for the nano-multilayer $(TiN/ZrN)_n$ deposited by PVD methods, it has been shown that a decrease in the bilayer thickness leads to significant grain refinement, an increase in microhardness, and the formation of wear tracks that are more resistant to wear and delamination; at the same time, in the work of Gonzalez-Carmona et al. it was emphasized that the multilayer architecture of TiN/ZrN provides higher resistance to local coating degradation compared with monolithic TiN and ZrN, which is directly related to the effective damping of stresses at the interlayer boundaries [7].

A similar approach has been implemented for WN-based multilayer systems WN/MeN (Me = Zr, Cr, Mo, Nb), where the introduction of a second nitride layer made it possible to form a nanocomposite structure with high hardness (more than 30 GPa), low specific wear, and stable performance under sliding friction; the authors showed that optimization of the thickness and sequence of WN/MeN layers makes it possible to maintain high load-bearing capacity and prevent premature spallation even under increased contact loads, which indicates the realization of so-called “architectural strengthening” also under adhesion-loaded conditions [8].

Particular attention is attracted by systems based on TiN and NbN, which are close in composition to our Ti–Mo–Nb-containing coatings: Sugumaran et al. demonstrated that a nanoscale TiN/NbN multilayer deposited using HIPIMS-UBM on a CoCrMo alloy forms an extremely dense structure free of intercolumnar pores with a hardness of ~ 28 GPa, a low coefficient of friction, and high critical loads in the scratch test, which the authors associate with the combination of intensive ion pre-treatment of the substrate and the superlattice structure of the coating [9]. Further analysis of TiN/NbN superlattices showed that under localized loading individual nanolayers can collectively rearrange without destruction of the integrity of the film; at the same time, focused ion beam cross-sections demonstrated very strong adhesion of the coating to the CoCrMo substrate, which the authors interpret as a consequence of the controlled formation of a graded transition layer and a high density of defects at the “substrate/first layer” interface [10].

Thus, modern studies of multilayer nitride systems – from $(TiN/ZrN)_n$ to WN/MeN and TiN/NbN – consistently indicate that the rational selection of pairs of transition metal nitrides (in particular based on Ti, Mo, Nb), control of the bilayer thickness, and the energy of the ion flux during deposition make it possible not only to increase hardness and wear resistance but also to ensure high adhesion characteristics that are critical for the long-term operation of protective coatings in contact-loaded components [7–11].

The evolution of multilayer nitride systems is not limited only to the combination of binary compounds; in recent years, considerable attention has been paid to architectures that combine binary and ternary nitrides, allowing even more flexible control of the mechanical and adhesive properties of coatings. For example, in multilayer systems of the type $(TiZrN)/NbN$, it has been established that the introduction of NbN layers into the structure of ternary TiZrN leads to the formation of a denser microstructure with increased crack resistance, and the critical loads L_c during scratch testing increase due to the optimal distribution of residual stresses between the layers [12]. Similarly, in TiSiN/CrN multilayers, it has been shown that the presence of Si in the upper layers forms amorphized barrier zones and reduces the probability of brittle cracking, while CrN provides a high load-bearing capacity of the interface; as a result, the system demonstrates increased adhesion strength and delayed initiation of delamination in the contact zone [13]. In addition, in works devoted to TiCrN/NbN and TiCrN/MoN multilayers, it has been established that the combination of hard and thermally stable TiCrN with more plastic NbN or oxide-forming MoN allows reduction of the concentration of local stresses and increases resistance to microcrack formation, which directly correlates with adhesion strength under conditions of increasing load [14].

A comprehensive analysis of the available literature data shows that although multilayer coatings combining binary and ternary nitrides demonstrate significant advantages over classical systems, the TiMoN/NbN combination remains practically unexplored, specifically in terms of adhesive properties. In the available sources, there are no systematic studies on the influence of technological parameters on the critical loads of delamination, failure mechanisms, and adhesive behavior of such multilayers. Therefore, the aim of this work is the experimental investigation of the adhesion characteristics of the multilayer TiMoN/NbN coating, focused on the influence of the working pressure during cathodic arc deposition (0.52 Pa and 0.13 Pa) on the formation of the interface and the failure patterns under localized mechanical loading.

2. EXPERIMENTAL DETAILS

2.1. Deposition

Multilayer TiMoN/NbN coatings were deposited by the cathodic arc evaporation method (CAE-PVD) using two cathodes: a Ti–Mo alloy with a ratio of 80:20 and high-purity niobium (Nb). The deposition was carried out in a vertical-type vacuum chamber equipped with a reactive gas flow control system and automatic switching of the arc between the cathodes. Before coating deposition, AISI 304 steel substrates underwent standard preparation: ultrasonic cleaning in an organic solvent, followed by Ar⁺ ion etching at a high negative bias to remove oxide films and improve adhesion of the initial layer.

The coatings were formed as a multilayer structure by alternating evaporation of the Ti–Mo and Nb cathodes. The arc current was 110 A for the TiMo cathode and 90 A for the Nb cathode. High-purity nitrogen was used as the working reactive gas, and the pressure in the chamber during deposition was varied between two regimes: 0.52 Pa and 0.13 Pa, which made it possible to obtain two types of samples: 1-TiMoN/NbN and 2-TiMoN/NbN, respectively. The substrate bias voltage during deposition was –200 V, which ensured increased kinetic energy of ions and the formation of a dense structure of the nitride layers. The process duration was 90 min, resulting in a total coating thickness of 10–11 μm.

The number of formed layers was approximately 270, which corresponds to a superlattice regime with a period of several tens of nanometers. The process parameters and synthesis conditions of the investigated coatings are presented in Table 1 for convenience of comparison.

Table 1. Deposition parameters of the multilayer TiMoN/NbN coatings

Coating definition	Arc current Ti–Mo/Nb, A	Substrate bias, V	Nitrogen pressure, Pa	Deposition time, min	Thickness, μm
1-TiMoN/NbN	110/90	–200	0.52	90	9.5
2-TiMoN/NbN			0.13		

2.2. Characterization

The surface and cross-sectional microstructure at multiple magnifications, as well as the morphology of the surfaces after scratch testing, were characterized using a field-emission scanning electron microscope, FEI Nova NanoSEM 450. The acquired images were used to assess the surface morphology, the distribution of macroparticles, the growth characteristics, the multilayer architecture, and to determine the thickness and uniformity of the individual nanolayers.

Scratch adhesion tests were conducted using a Bruker UMT-2 tribometer under progressive loading. During the test, the normal load was gradually increased from 0.2 N to 46 N along a scratch length of approximately 5 mm over 50 s. This progressive loading mode allowed the identification of the critical loads corresponding to the onset of coating failure. The first critical load (L_{c1}) was associated with the appearance of buckling cracks, while the second critical load (L_{c2}) corresponded to buckling spallation, indicating local coating delamination.

After the scratch tests, the morphology of the scratch tracks was examined using a field-emission scanning electron microscope (Quanta 600 FEG) to analyze the failure mechanisms and damage evolution within the coating. To further investigate the compositional changes along the scratch tracks, energy-dispersive X-ray spectroscopy (Oxford Instruments high-performance SDD (Silicon Drift Detector)) analysis was performed at several characteristic locations.

3. EXPERIMENTAL RESULTS

3.1. Surface and cross-sectional structure

SEM analysis of the surface of multilayer TiMoN/NbN coatings presented in Figure 1 shows a morphology characteristic of coatings obtained by the cathodic arc deposition method. For both samples, the surface consists of a compact and continuous coating matrix, on which a significant number of spherical macroparticles (macroparticles or droplets) are observed. Such particles are formed as a result of the emission of molten fragments of the cathode material during cathodic arc evaporation and are a typical feature of this deposition method.

The surface of the multilayer 1-TiMoN/NbN coating, deposited at a nitrogen pressure of 0.52 Pa, is characterized by a relatively smooth morphology with a moderate amount of the droplet phase. In the SEM image, spherical macroparticles of different sizes are observed, unevenly distributed over the coating surface. Most particles have a diameter in the range of approximately 1–5 μm, which is typical for cathodic arc coatings.

The surface of the multilayer 2-TiMoN/NbN coating, deposited at a lower nitrogen pressure of 0.13 Pa, demonstrates a significantly different morphology. The SEM image shows a much higher density of the droplet phase, and the macroparticles exhibit a wide size distribution, ranging from submicron to several micrometers. The coating surface appears more “saturated” with macroparticles, which are located closer to each other and form a more heterogeneous

surface topography. In addition to large particles, a considerable number of smaller particles are also observed, which may be the result of macroparticle fragmentation or secondary deposition of material.

The revealed difference in the morphology of the coatings is related to the influence of the working gas pressure on the transport and energy of plasma particles during cathodic arc deposition. At a lower nitrogen pressure (0.13 Pa), the mean free path of particles in the plasma increases, leading to more rectilinear transport of macroparticles from the cathode to the substrate. Under such conditions, macroparticles have a lower probability of collisions with gas molecules and, accordingly, are less decelerated in the plasma. This promotes their more efficient transfer to the substrate surface and, consequently, increases the amount of the droplet phase on the coating surface.

Conversely, at higher nitrogen pressure (0.52 Pa), the number of collisions between macroparticles and gas molecules increases. Such collisions may lead to partial deceleration or even deviation of macroparticle trajectories in the plasma, thereby reducing the probability of their deposition on the substrate surface. As a result, the coating surface becomes smoother and contains less of the droplet phase.

Such changes in morphology may significantly influence the service properties of the coating. Macroparticles may act as stress concentrators during mechanical loading and affect the tribological behavior of the coating. At the same time, the presence of the droplet phase may also influence the processes of crack initiation during scratch testing.

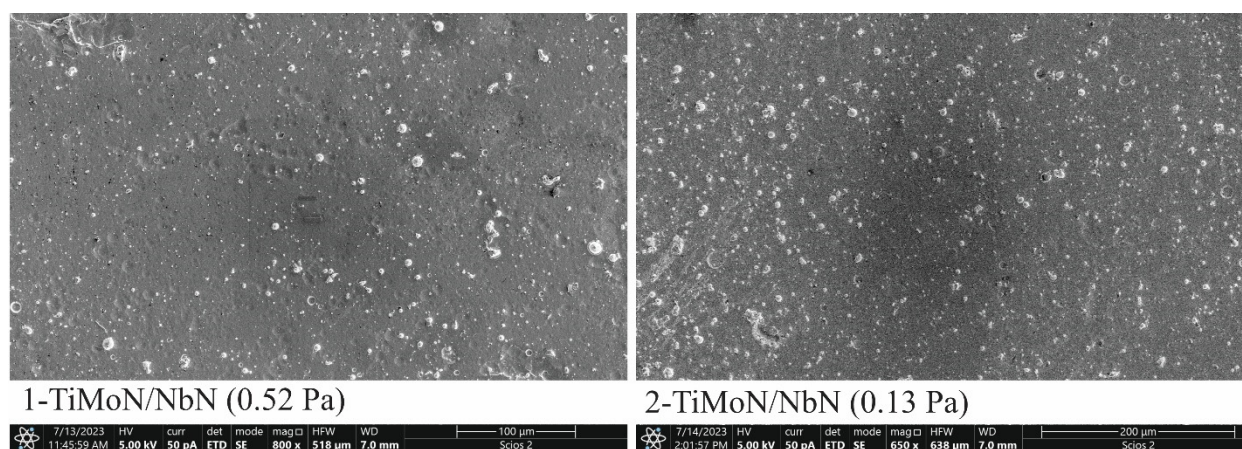


Figure 1. SEM images showing the surface morphology of the multilayer TiMoN/NbN coatings deposited at different nitrogen pressures

The cross-sectional SEM images presented in Figure 2 reveal that both investigated coatings exhibit a well-defined multilayer architecture characteristic of nanolayered nitride systems deposited by cathodic arc PVD. The coatings clearly consist of alternating light and dark layers corresponding to TiMoN and NbN constituents, respectively. Such contrast is typical due to differences in atomic number and electron scattering between the two phases. Apparently, the lighter layers correspond to the TiMoN phase, while the darker layers represent NbN. The multilayer sequence is continuous throughout the entire coating thickness, demonstrating a stable deposition process during cathodic arc evaporation. The interfaces between adjacent layers are well defined and nearly planar, indicating a relatively stable growth regime during deposition without significant interface roughening or intermixing. Moreover, both coatings exhibit a compact morphology with no visible pores, voids, or macroparticle inclusions in the cross-section, indicating a dense microstructure typical of energetic PVD deposition conditions. Measurements performed directly from the cross-sectional SEM images show that the overall coating thickness is approximately 9.5 μm for both coatings. Based on the periodic repetition of the alternating layers, the modulation period of the multilayer structure was estimated to be approximately 85 nm. This value corresponds to the combined thickness of one TiMoN layer and one NbN layer. Such nanoscale modulation is typical for multilayer nitride coatings designed to exploit superlattice-type strengthening effects.

The cross-section of the multilayer 1-TiMoN/NbN coating, deposited at a nitrogen pressure of 0.52 Pa, shows that the periodicity of the alternating layers is relatively uniform throughout the coating thickness. However, it is evident that the NbN layers are noticeably thicker than the TiMoN layers. This asymmetry in the thickness of the constituent layers apparently indicates that the effective deposition rate of NbN during the multilayer growth was higher than that of TiMoN. In cathodic arc deposition processes, the layer thickness in a multilayer coating is primarily determined by the deposition rate of each cathode material. Therefore, the thicker NbN layers observed in this coating most likely reflect either a higher plasma flux from the Nb cathode. Moreover, the interfaces between layers remain relatively smooth and continuous, which suggests that the growth process proceeded under stable plasma conditions. The multilayer architecture is preserved throughout the entire coating thickness, with no evidence of structural disruption, indicating high stability of the deposition process under a nitrogen pressure of 0.52 Pa.

The cross-section of the multilayer 2-TiMoN/NbN coating, deposited at a lower nitrogen pressure of 0.13 Pa, also exhibits a clearly defined multilayer architecture. The layer interfaces remain sharp and continuous, indicating that the reduction of nitrogen pressure did not disrupt the formation of the multilayer structure. However, in contrast to the coating deposited at 0.52 Pa, the relative thicknesses of the constituent layers appear more balanced in this sample. The NbN and TiMoN layers appear to be closer in thickness than the multilayer 1-TiMoN/NbN coating, although the NbN layers are still

slightly thicker. Apparently, the decrease in nitrogen pressure may influence the effective deposition kinetics of the different metal species in the plasma. Under lower nitrogen pressure conditions, the mean free path of plasma species increases, which can modify the arrival rate of metal ions at the growing surface. Such changes may affect the growth rates of the individual layers and, therefore, the relative thicknesses of the TiMoN and NbN layers within the multilayer sequence. Despite these differences, the multilayer architecture remains well preserved, and the coating retains a dense structure throughout the thickness. Evidently, the energetic conditions of cathodic arc deposition promote strong atomic mobility at the growing surface, allowing the formation of well-defined nanolayers even when the nitrogen pressure is reduced.

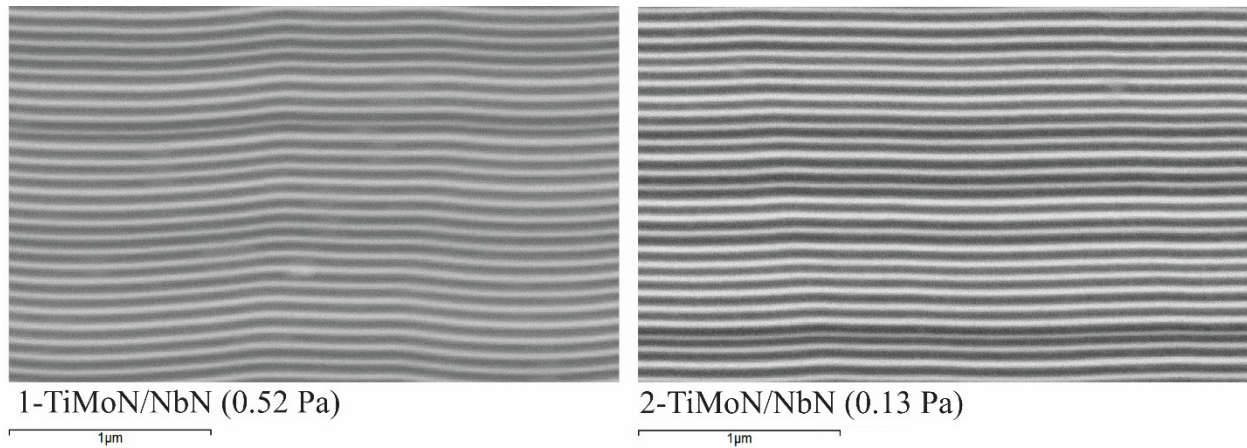


Figure 2. Cross-sectional SEM images of the multilayer TiMoN/NbN coatings deposited at different nitrogen pressures

This observation suggests that the nitrogen pressure influences the growth kinetics of the multilayer TiMoN/NbN system, possibly through changes in plasma density, ionization efficiency, and the effective deposition rates of the individual cathode materials. Such variations in layer thickness can affect the mechanical behaviour of multilayer coatings, as the modulation period and layer-thickness ratio are known to influence dislocation blocking and crack propagation mechanisms in nanolayered nitride coatings.

3.2. Scratch test damage morphology and compositional evolution

Scratch testing is one of the most informative methods for assessing the adhesion strength of hard coatings, as it allows investigation of the mechanisms of their failure under gradually increasing loads. The morphology of the scratch tracks obtained during progressive-load scratch testing provides important insights into the adhesion behaviour and failure mechanisms of the multilayer TiMoN/NbN coatings. SEM observations of the damaged surfaces, presented in Figure 3, reveal distinct deformation and fracture features associated with the critical loads L_{c1} (buckling cracks) and L_{c2} (buckling spallation) identified during the test. The coatings were tested under progressive loading conditions, which allowed gradual development of failure processes within the coating–substrate system.

The scratch track formed on the multilayer 1-TiMoN/NbN coating, deposited at a nitrogen pressure of 0.52 Pa, exhibits a relatively well-defined damage morphology. At the initial region of the track, the coating remains largely intact, while with increasing load, the first signs of coating instability become visible in the form of lateral cracks located near the edges of the groove. Apparently, the first critical failure event corresponds to buckling cracks occurring at $L_{c1} \approx 4.72$ N. These cracks appear primarily along the edges of the scratch track, where tensile stresses develop during coating bending as the substrate plastically deforms beneath the indenter. Evidently, the cracks propagate parallel to the sliding direction, which is characteristic of compressively stressed PVD coatings undergoing local buckling instability. With further increase of the load, larger damaged regions become visible. The central region of the track shows a relatively compact wear scar, while partial coating detachment is observed along the edges of the groove. This behaviour corresponds to the second critical load, $L_{c2} \approx 12.38$ N, associated with buckling spallation. In this stage, the previously formed buckled segments lose adhesion to the substrate and detach locally, forming flake-like fragments adjacent to the scratch groove. Moreover, the damage morphology indicates that the coating failure progresses gradually rather than catastrophically. The coating still remains partially attached to the substrate within the track, suggesting a relatively high adhesion strength of the multilayer structure.

The scratch track observed on the multilayer 2-TiMoN/NbN coating, deposited at a lower nitrogen pressure of 0.13 Pa, shows a somewhat different morphology. The groove appears slightly smoother and more continuous along the sliding direction, while the surrounding regions exhibit a more pronounced accumulation of plastically deformed coating material. Apparently, the first cracking event occurs at a slightly higher load, $L_{c1} \approx 5.41$ N, indicating somewhat improved resistance to the onset of buckling compared with the coating deposited at the higher nitrogen pressure. The cracks again originate at the edges of the scratch track, where tensile stresses develop due to substrate deformation. However, the damage pattern differs from that observed in the first coating. In this sample, the coating fragments tend to form periodic arcuate features along the groove edges. These structures resemble successive buckling segments that have partially detached and folded during sliding. Such morphology is typical for multilayer coatings undergoing progressive buckling-

induced delamination. The second critical event, $L_{c2} \approx 12.54$ N, corresponding to buckling spallation, occurs at a load very similar to that observed for the first coating. At this stage, segments of the coating detach from the substrate and accumulate near the edges of the scratch track.

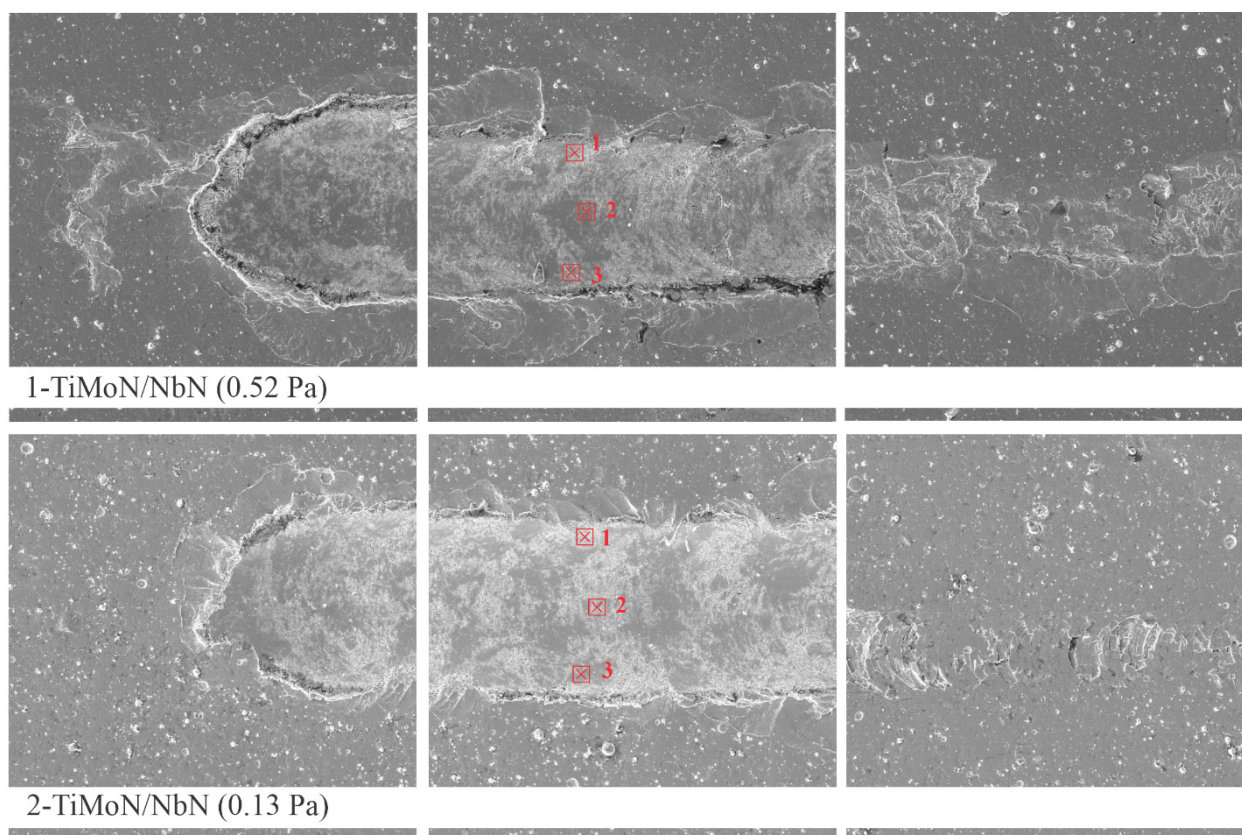


Figure 3. SEM images of the scratch tracks formed during progressive load scratch testing of the multilayer TiMoN/NbN coatings deposited at different nitrogen pressures. The locations of EDS analysis (Spectrum 1–3) are indicated

To evaluate the compositional changes within the scratch track, EDS measurements were carried out at three characteristic locations, namely at the upper edge of the groove (Spectrum 1), in the center of the groove (Spectrum 2), and at the lower edge of the groove (Spectrum 3), with the obtained elemental compositions presented in Table 2.

Table 2. Elemental composition of the scratch track regions obtained by EDS analysis for the multilayer TiMoN/NbN coatings deposited at different nitrogen pressures

Coating	Atomic %						
	O	Al	Ti	Cr	Fe	Nb	Mo
1-TiMoN/NbN							
Spectrum 1	6.46	0.30	22.26	7.04	23.66	34.76	5.53
Spectrum 2	2.27	0.72	3.19	14.67	73.65	4.71	0.66
Spectrum 3	20.57	1.11	36.24	1.32	4.89	31.55	4.28
Mean	9.76	0.71	20.56	7.68	34.07	23.67	3.49
2-TiMoN/NbN							
Spectrum 1	16.58	0.50	45.81	0.68	1.56	23.10	11.78
Spectrum 2	19.04	0.84	44.82	0.79	3.27	26.53	4.71
Spectrum 3	12.14	0.56	39.99	2.78	11.63	28.53	4.36
Mean	15.55	0.67	34.17	4.22	19.84	20.73	4.79

The EDS results reveal significant compositional variations across the scratch track. At the upper edge of the track (Spectrum 1), the multilayer 1-TiMoN/NbN coating composition is dominated by Nb (34.76 at.%) together with Ti (22.26 at.%) and Fe (23.66 at.%). The presence of Fe clearly indicates that the substrate material is partially exposed or mixed with the coating debris during scratching. In the center of the groove (Spectrum 2), the composition is strongly dominated by Fe (73.65 at.%). This evidently indicates that the coating has been largely removed in this region, and the steel substrate is exposed. Only small amounts of Ti, Nb, and Mo remain, which likely originate from residual coating fragments or wear debris. At the lower edge of the track (Spectrum 3), the Nb and Ti contents increase again (31.55 and 36.24 at.% respectively), while the Fe concentration drops significantly. This observation suggests that coating fragments accumulate at the edges of the scratch track during the spallation process.

A somewhat different compositional trend is observed for the multilayer coating deposited at lower nitrogen pressure. At the upper edge of the groove (Spectrum 1), the Ti concentration is particularly high (≈ 45.81 at.%), accompanied by Nb (23.10 at.%) and Mo (11.78 at.%). The Fe content is very low (≈ 1.56 at.%), indicating that the coating remains largely intact in this region. In the center of the scratch track (Spectrum 2), Ti remains the dominant element (~ 44.82 at.%), while Nb and Mo are also present. Only a small amount of Fe (3.27 at.%) is detected, suggesting that the substrate exposure is significantly lower than in the coating deposited at 0.52 Pa. At the lower edge of the track (Spectrum 3), the Fe content increases to about 11.63 at.%, while Ti and Nb remain substantial. This indicates partial removal of the coating, accompanied by mixing of coating fragments with substrate material.

The comparison of the EDS results clearly indicates that the multilayer 1-TiMoN/NbN coating, deposited at a nitrogen pressure of 0.52 Pa, experiences more extensive exposure of the substrate within the center of the scratch track, as evidenced by the very high Fe concentration (≈ 73 at.%). In contrast, the multilayer 2-TiMoN/NbN coating, deposited at a lower nitrogen pressure of 0.13 Pa, retains a much higher fraction of the coating material within the track because the Fe concentration remains relatively low. Apparently, this suggests that the coating deposited at lower nitrogen pressure exhibits slightly improved resistance to complete coating removal during scratching.

The SEM observations combined with the EDS compositional analysis suggest that different failure modes dominate in the multilayer TiMoN/NbN coatings. In the 1-TiMoN/NbN coating, the very high Fe concentration detected at the center of the scratch track (≈ 73 at.% Fe) evidently indicates complete removal of the coating, exposing the steel substrate. Such damage morphology suggests that the failure is largely adhesive, occurring at the coating–substrate interface and resulting in local coating delamination.

In contrast, the multilayer 2-TiMoN/NbN coating exhibits a markedly lower Fe concentration within the scratch track, while Ti, Nb, and Mo remain the dominant elements. Apparently, this indicates that a significant portion of the coating remains inside the groove. The observed fragmentation and plastic deformation of the coating without full substrate exposure suggests that the failure mode is predominantly cohesive, occurring within the multilayer structure rather than at the coating–substrate interface.

4. DISCUSSIONS

The described results demonstrate that by varying the working gas pressure during CAE-PVD deposition, it is possible to deliberately control the adhesion behaviour of multilayer TiMoN/NbN coatings. The difference in the onset of buckling cracks between the two coatings may be related to the influence of nitrogen pressure on the microstructure formed during deposition. The pressure of the working gas during coating deposition can significantly affect the mechanisms of buckling-related failure. Lower nitrogen pressure generally leads to higher kinetic energy of the depositing species, since the mean free path of plasma particles increases and fewer collisions occur in the plasma.

Under such conditions, the arriving metal ions possess higher energy, which promotes enhanced ion bombardment of the growing surface and leads to the formation of a denser coating microstructure with improved adhesion to the substrate. As a consequence, the initiation of buckling cracks may occur at higher applied loads, while buckling spallation is observed only after significant accumulation of deformation within the coating–substrate system.

Apparently, the multilayer coating deposited at a lower nitrogen pressure of 0.13 Pa exhibits slightly improved resistance to crack initiation, as reflected by the higher L_{c1} value (5.41 N) than that of the multilayer coating deposited at a higher nitrogen pressure of 0.52 Pa (4.72 N). Conversely, when the nitrogen pressure is higher, the energy of depositing species may decrease due to more frequent collisions in the plasma, which can result in the formation of a comparatively less dense coating structure. Under such conditions, interfacial stresses may accumulate more rapidly, leading to the earlier onset of coating detachment during scratch loading.

However, the second critical load corresponding to buckling spallation remains very similar for both coatings ($L_{c2} \approx 12.4$ – 12.5 N), indicating that the ultimate adhesion strength of the coatings is comparable despite the differences in the initial crack initiation behaviour.

CONCLUSIONS

Multilayer TiMoN/NbN coatings with a nanolayered architecture were successfully deposited by cathodic arc PVD at nitrogen pressures of 0.52 Pa and 0.13 Pa. Both coatings exhibit a dense multilayer structure consisting of alternating TiMoN and NbN layers with a modulation period of approximately 85 nm and an overall thickness of about 9.5 μm .

Surface SEM observations revealed a typical cathodic arc morphology characterized by the presence of macroparticles. A decrease in nitrogen pressure leads to an increased density of macroparticles due to the longer mean free path of plasma species during deposition.

Scratch testing under progressive loading conditions identified two characteristic failure events corresponding to buckling crack initiation (L_{c1}) and buckling spallation (L_{c2}). The multilayer coating deposited at a lower nitrogen pressure of 0.13 Pa shows slightly higher resistance to crack initiation ($L_{c1} \approx 5.41$ N) compared with the multilayer coating deposited at 0.52 Pa ($L_{c1} \approx 4.72$ N).

SEM and EDS analyses of the scratch tracks revealed distinct failure modes in the investigated coatings. The coating deposited at 0.52 Pa exhibits predominantly adhesive failure associated with exposure of the steel substrate, whereas the coating deposited at 0.13 Pa demonstrates mainly cohesive failure within the multilayer structure.

The obtained results indicate that nitrogen pressure during cathodic arc deposition plays an important role in controlling the microstructure evolution and adhesion behaviour of TiMoN/NbN multilayer coatings.

Acknowledgments

This work was supported by the Ministry of Education and Science of Ukraine (MES) under the National Budget Program (Project 0124U001127).

ORCID

Olga Maksakova, <https://orcid.org/0000-0002-0646-6704>; Vyacheslav Beresnev, <https://orcid.org/0000-0002-4623-3243>
 Serhiy Lytovchenko, <https://orcid.org/0000-0002-3292-5468>; Martin Sahul, <https://orcid.org/0000-0001-9472-500X>
 Mária Čaplovičová, <https://orcid.org/0000-0003-4767-8823>; Ruslan Galushkov, <https://orcid.org/0000-0002-9105-9774>

REFERENCES

- [1] J. Xu, *et al.*, “Tribological Properties of MoN/TiN Multilayer Coatings Prepared via High-Power Impulse Magnetron Sputtering,” *Lubricants*, **13**(8), 319 (2025). <https://doi.org/10.3390/lubricants13080319>
- [2] T. Borowski, *et al.*, “Influence of Magnetron Sputtering-Deposited Niobium Nitride Coating and Its Thermal Oxidation on the Properties of AISI 316L Steel in Terms of Its Medical Applications,” *Materials*, **16**, 6890 (2023). <https://doi.org/10.3390/ma16216890>
- [3] J. Chen, *et al.*, “Excellent Anti-Corrosion and Conductivity of NbN Coated on Ti Bipolar Plate by Controlling N₂ Flow Rates,” *Journal of Alloys and Compounds*, **976**, 173033 (2024). <https://doi.org/10.1016/j.jallcom.2023.173033>
- [4] J.M. Gonzalez-Carmona, *et al.*, “TiNbN Hard Coating Deposited at Varied Substrate Temperature by Cathodic Arc: Tribological Performance under Simulated Cutting Conditions,” *Materials*, **16**, 4531 (2023). <https://doi.org/10.3390/ma16134531>
- [5] T. Borowski, *et al.*, “Properties of Oxidised NbN Coating Produced by Magnetron Sputtering on AISI 316L Steel in View of Its Biomedical Applications,” SSRN preprint, (2023). <https://doi.org/10.2139/ssrn.4391424>
- [6] J. Van Meter, *et al.*, “Wear and Adhesion of PEALD Titanium Molybdenum Nitrides (TiMoN) Films,” *Wear*, **570**, 205980 (2025). <https://doi.org/10.1016/j.wear.2025.205980>
- [7] J.M. González-Carmona, *et al.*, “Wear mechanisms identification using Kelvin probe force microscopy in TiN, ZrN, and TiN/ZrN hard ceramic multilayer coatings,” *Ceramics International*, **46**(15), 24592–24604 (2020). <https://doi.org/10.1016/j.ceramint.2020.06.248>
- [8] K. Smymova, *et al.*, “Microstructure, Mechanical and Tribological Properties of Advanced Layered WN/MeN (Me = Zr, Cr, Mo, Nb) Nanocomposite Coatings,” *Nanomaterials*, **12**(3), 395 (2022). <https://doi.org/10.3390/nano12030395>
- [9] A.A. Sugumaran, *et al.*, “TiN/NbN Nanoscale Multilayer Coatings Deposited by High Power Impulse Magnetron Sputtering to Protect Medical-Grade CoCrMo Alloys,” *Coatings*, **11**(7), 867 (2021). <https://doi.org/10.3390/coatings11070867>
- [10] P.E. Hovsepian, *et al.*, “Microstructure and load-bearing capacity of TiN/NbN superlattice coatings deposited on medical-grade CoCrMo alloy by HIPIMS,” *Journal of the Mechanical Behavior of Biomedical Materials*, **132**, 105267 (2022). <https://doi.org/10.1016/j.jmbbm.2022.105267>
- [11] Y. Liu, *et al.*, “Multilayer Coatings for Tribology: A Mini Review,” *Nanomaterials*, **12**(9), 1388 (2022). <https://doi.org/10.3390/nano12091388>
- [12] O. Maksakova, *et al.*, “A Comparative Study of Microstructure and Properties of TiZrN/NbN and TiSiN/NbN Nanolaminate Coatings,” in: *Nanocomposite and Nanocrystalline Materials and Coatings. Advanced Structured Materials*, edited by A.D. Pogrebnjak, Y. Bing, and M. Sahul, vol 214. (Springer, Singapore, 2024). https://doi.org/10.1007/978-981-97-2667-7_6
- [13] S.-M. Yang, *et al.*, “Microstructure Characterization of Multilayered TiSiN/CrN Thin Films,” *Journal of Nanoscience and Nanotechnology*, **8**(5), 2688–2692 (2008). <https://doi.org/10.1166/jnn.2008.592>
- [14] Y. Liu, *et al.*, “Multilayer Coatings for Tribology: A Mini Review,” *Nanomaterials*, **12**, 1388 (2022). <https://doi.org/10.3390/nano12091388>

ВПЛИВ ТИСКУ АЗОТУ НА АДГЕЗІЮ ТА МЕХАНІЗМИ РУЙНУВАННЯ ПРИ СКРЕТЧ-ТЕСТУВАННІ БАГАТОШАРОВИХ ПОКРИТТІВ TiMoN/NbN, ОСАДЖЕНИХ МЕТОДОМ КАТОДНО-ДУГОВОГО PVD

O.B. Maksakova¹, V.M. Beresnev¹, S.V. Lytovchenko¹, M. Sahul², M. Čaplovičová³, R.S. Galushkov¹

¹Харківський національний університет імені В.Н. Каразіна, майд. Свободи, 4, 61000 Харків, Україна

²Інститут матеріалознавства, Словацький технологічний університет у Братиславі, вул. Яна Ботту, 25, 917 24, Трнава, Словаччина

³Центр нанодіагностики матеріалів, Словацький технологічний університет у Братиславі, вул. Вазовова, 5, 812 43, Братислава, Словаччина

Багатошарові нітридні покриття широко використовуються для покращення механічних властивостей і довговічності інженерних компонентів, що працюють в умовах інтенсивного трибологічного навантаження. У цій роботі досліджено адгезійну поведінку та механізми руйнування багатошарових покриттів TiMoN/NbN, осаджених методом катодно-дугового PVD, залежно від робочого тиску азоту. Два покриття були синтезовані при тисках азоту 0,52 Па та 0,13 Па за інших однакових умов осадження. Мікроскопічний аналіз показав, що обидва покриття мають добре виражену наношарову архітектуру, що складається з чергування шарів TiMoN та NbN з періодом модуляції приблизно 85 нм і загальною товщиною близько 9,5 мкм. Зменшення тиску азоту призводить до більшої густини макрочасток через більшу довжину вільного пробігу плазмових частинок катодно-дугового розряду. Скретч-тести адгезії, виконані в умовах поступового збільшення навантаження, дозволили ідентифікувати дві характерні події руйнування, що відповідають зародженню тріщин та відшаруванню, що спричинені втрачанням стійкості. Багатошарове покриття, осаджене при 0,13 Па, продемонструвало дещо кращу стійкість до зародження тріщин (5,41 Н) порівняно з багатошаровим покриттям, осадженим при 0,52 Па (4,72 Н). Однак обидва покриття демонстрували подібні значення другого критичного навантаження (12,4–12,5 Н). Багатошарове покриття, осаджене при вищому тиску азоту, переважно зазнає адгезійного руйнування з інтенсивним оголенням підкладки, тоді як багатошарове покриття, осаджене при нижчому тиску азоту, демонструє переважно когезійні пошкодження всередині багатошарової структури. Отримані результати демонструють, що тиск азоту під час катодно-дугового осадження суттєво впливає на еволюцію мікроструктури та механізми адгезійного руйнування в багатошарових покриттях TiMoN/NbN. Дослідження надає уявлення щодо оптимізації параметрів осадження для покращення механічної надійності багатошарових нітридних покриттів.

Ключові слова: вакуумно-дугова технологія; нітриди; багатошарові покриття; TiMoN; мікроструктура; склад; адгезія